

Redefining the dielectric response of nanoconfined liquids: insights from water

Jon Zubeltzu,¹ Fernando Bresme,² Matthew Dawber,³ Marivi Fernandez-Serra,³ and Emilio Artacho^{4,5,6}

¹*Department of Applied Physics, Engineering School of Gipuzkoa,*

Basque Country University, UPV-EHU, Europa Plaza 1, 20018 San Sebastian, Spain.

²*Department of Chemistry, Molecular Sciences Research Hub, Imperial College London,
London W12 0BZ, United Kingdom and Thomas Young Centre for Theory and Simulation of Materials,
Imperial College London, London SW7 2AZ, United Kingdom*

³*Department of Physics and Astronomy, Stony Brook University, New York 11794-3800, USA*

⁴*CIC Nanogune BRTA and DIPC, Tolosa Hiribidea 76, 20018 San Sebastian Spain*

⁵*Ikerbasque, Basque Foundation for Science, 48011 Bilbao, Spain*

⁶*Theory of Condensed Matter, Cavendish Laboratory, University of Cambridge,
J. J. Thomson Ave, Cambridge CB3 0HE, United Kingdom*

(Dated: December 3, 2024)

Recent experiments show that the relative dielectric constant ϵ of water confined to a film of nanometric thickness reaches a strikingly low value of 2.1, barely above the bulk's 1.8 value for the purely electronic response. We argue that ϵ is not a well-defined measure for dielectric properties at sub-nanometer scales due to the ambiguous definition of confinement width. Instead we propose the 2D polarisability α_{\perp} as the appropriate, well-defined response function whose magnitude can be directly obtained from both measurements and computations. Our molecular-dynamics computations based on density-functional theory and empirical force fields reproduce the previously reported low dielectric response of confined water, and importantly predict a very significant reduction, $\sim 30\%$, of the electronic response as compared with the bulk's, contrary to what is widely assumed, highlighting the importance of electronic degrees of freedom to interpret the dielectric response of polar fluids under nanoconfinement conditions.

The relative dielectric constant ϵ_{\perp} across a nanometric thin film of water was recently measured to be as low as 2.1 for a width of $w \lesssim 1$ nm. This paper by Fumagalli *et al.* [1] attracted enormous attention for two main reasons: (i) it is a beautiful, impressive *tour-de-force* experiment, and (ii) the mentioned value is strikingly low, barely above the water bulk's purely electronic response [2] $\epsilon_{\infty}^b = 1.8$. The first point is undisputed. It is the second one we want to qualify in this article.

A small value for ϵ_{\perp} is not a surprising result. Numerous simulations have already shown that values in the $\epsilon_{\perp} < 10$ range are to be expected for confined water geometries [3–7]. The explanation of the origin of such reduced value appearing in several works [8–10] after that of Fumagalli *et al.* [1], including high-quality calculations (see e.g. Ref. 9), agree, in essence, with the earlier literature, all based on a combination of a more rigid structure of the water layer close to the interface [3–6], and the dead-layer effect (capacitors in series) for the thickness dependence [7]. Alternatively, in a recent work, it was proposed that the dielectric permittivity reduction of water is not connected to the structural alignment of interfacial water molecules, and instead, it emerges from anisotropic long range dipole correlations next to surfaces [11]. The reduction of the dielectric permittivity in other H-bonded and non H-bonded solvents was discussed recently [12], highlighting the generality of the observed reduction of the dielectric permittivity under confinement conditions.

The impact of interfaces on the permittivity tensor of water has attracted significant attention, which has stim-

ulated the use of the dielectric tensor as a local function explicitly quantifying its dependence on the distance to the interface using statistical mechanics fluctuation formula [10, 11, 13, 14]. These studies already showed that major changes in the dielectric response of water appear at distances < 1 nm from a surface, demonstrating the anisotropy of the permittivity tensor, the relevance of the surface-water interactions in determining the permittivity, and the importance of interfacial layers in defining the dielectric response of interfacial water. Despite the intrinsic interest of calculating the spatial dependence of the dielectric permittivity profile, its interpretation in mesoscopic and molecular scales is not straightforward, as it requires an averaging process over molecular layers [9–11]. Furthermore, while most studies focused on the modification of molecular degrees of freedom such as dipole-dipole correlations or water orientation at surfaces, the impact of confinement on electronic degrees of freedom has escaped scrutiny. One aspect of particular importance, which we address in our work, is whether confinement influences the electronic polarisability of confined water relative to bulk conditions. This is an important question, especially considering the very low permittivity of confined water inferred from experiments and theory. The importance of confinement effects and of molecular degrees of freedom has been discussed more widely in the investigation of fluid flow at the nanoscale. Advances in this area are promising, particularly in the development of novel devices with enhanced properties, which rely to some extent on the breakdown of the macroscopic theories that assume a continuum frame-

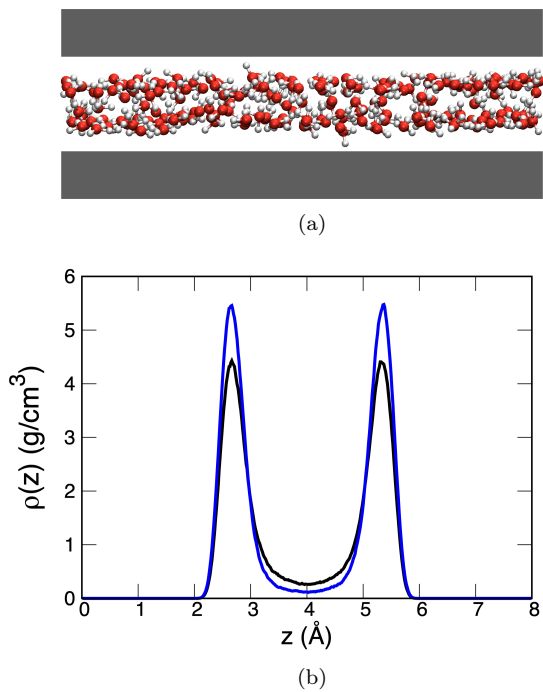


FIG. 1. (a) Schematic view of the simulation box, perpendicular to the confining plane. The gray-shaded regions represent the location of the confining soft potentials. Oxygen and hydrogen atoms in the water molecules are represented as red and white spheres, respectively. (b) Oxygen density profiles along the confining direction for 2D densities $\sigma = 0.177 \text{ \AA}^{-2}$ (black) and 0.195 \AA^{-2} (blue).

work [15]. We argue below that using macroscopically defined properties is also problematic when considering the electrostatic response of fluids under nanoconfinement conditions.

Our purpose here is not improving on the determination of ϵ_{\perp} but instead stating that it is an ill-defined quantity in the sub-nm regime, and that insisting on its quantification is misleading the discussion of the key variables determining the electrostatic screening of confined fluids. As noted above, a problem emerges when assigning a dielectric permittivity to a molecular layer. This calculation requires the definition of a layer thickness to integrate the local perpendicular dielectric permittivity. The minima of the water center of mass density profiles normal to the surface are often used to define such thickness. As discussed before [1, 9], the actual value of the computed or measured ϵ_{\perp} is rather arbitrary, as the result depends on establishing an effective film width w that cannot be uniquely defined. Hence, the definition of the film width becomes essentially the answer to an ill-posed question, which may have sensible answers but not observable ones. Think, e.g. asking what is the width of an isolated graphene sheet. In essence, this is a problem arising from carrying a macroscopic-theory language over to the sub-nm regime.

The dielectric constant, relating the polarisation P to the applied electric field, quantifies the response of a material within the macroscopic framework of Maxwell’s equations. It is P that is ill-defined due to the ambiguity in the width, as P is given by the dipole moment per unit volume. Instead, the corresponding characterization for a two-dimensional (2D) system is given by the dipole moment per unit area, \mathcal{P}_{2D} . We propose that for sub-nm thickness, the 2D description is the correct one to use, the cross-over from the 3D description being determined by the ambiguity in ϵ_{\perp} becoming comparable with the value itself. The transverse dielectric response is then characterized by the 2D transverse polarizability

$$\alpha_{\perp} \equiv \frac{1}{\epsilon_0} \frac{\partial \mathcal{P}_{2D}}{\partial \mathcal{E}_{\perp}^{\text{ext}}} \quad (1)$$

as already proposed for 2D materials [16], instead of the conventional susceptibility in 3D. As done for the polarizability of molecules in the gas phase, referring to the externally applied electric field $\mathcal{E}_{\perp}^{\text{ext}}$ is the obvious choice here since it makes no sense to refer to the perpendicular field inside a 2D system. For solid-state thin film systems, a “macroscopically averaged” electrostatic potential can be defined as a function of the perpendicular component [17], which is routinely used in interface and heterostructure physics. It has also been used in soft matter thin films (e.g. soap/water interfaces [18]), but the difficulty remains when averaging the field over an ill-defined width.

$\epsilon_0 \mathcal{E}_{\perp}^{\text{ext}}$ in vacuum equals the electric displacement field D_{\perp} to be used when P is well defined. The defined α_{\perp} has units of length and is analogous to the conventionally defined molecular polarisability, which has units of volume. It can be called the dielectric thickness of the film. It is important to remember key differences when referring to the external field instead of the internal. For that, the definition in Eq. (1) can be extended to 3D as $\epsilon_0 \alpha_{3D} \equiv \partial P / \partial \mathcal{E}^{\text{ext}}$, using the conventional 3D polarisation P . Both polarisabilities are related by $\alpha_{3D} = \alpha_{\perp} / w$ in the context of this work [19], since $P = \mathcal{P}_{2D} / w$. α_{3D} relates to the conventional relative dielectric constant as $\alpha_{3D} = 1 - \epsilon^{-1}$, which means that the range of 1 to ∞ for ϵ (from no response to complete screening of the internal field as in an ideal metal) becomes 0 to 1 for α_{3D} .

To illustrate the main ideas conveyed here, we present two sets of simulations for a bilayer liquid film of water confined along the z direction of the simulation box between two soft Lennard-Jones 9-3 separated by 8 \AA between their respective origins (see Figure 1). The parameters of the confining potential are set to mimic the interaction of water with solid paraffin [20]. This same system has been extensively studied in previous works [4, 20–24]. The bilayer film thickness is at the lower end of the systems measured in Ref. 1. For classical trajectories obtained using the empirical force field TIP4P/2005 [25] at $T = 300 \text{ K}$ under various values of an applied exter-

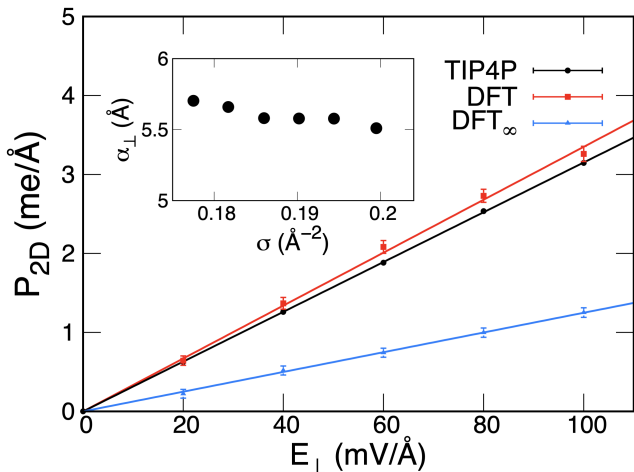


FIG. 2. 2D polarisation \mathcal{P}_{2D} vs external traverse electric field $\mathcal{E}_{\perp}^{\text{ext}}$ for TIP4P-2005 water classical trajectories (black) and for DFT calculations using the classical TIP4P-2005 under the same external field (red). In blue, we show the pure electronic response obtained from DFT as explained in the text. Inset: 2D density dependence of α_{\perp} obtained with the TIP4P-2005 classical simulations.

nal field, we calculate α_{\perp} from the \mathcal{P}_{2D} obtained from (i) the point charges of the TIP4P/2005 model and (ii) from the perpendicular dipole obtained with density-functional theory (DFT) on a sample of snapshots of the classical trajectory, under the same external electrostatic field values. The TIP4P/2005 trajectories are generated within the NVT ensemble using the Nosé-Hoover thermostat involving 10 ns of equilibration time followed by 10 ns of production time. The simulation box, with dimensions $34.39 \text{ \AA} \times 34.39 \text{ \AA} \times 23.00 \text{ \AA}$, contains between 210 and 236 water molecules. This corresponds to a 2D molecular density range of $0.177 \text{ \AA}^{-2} - 0.200 \text{ \AA}^{-2}$, where water is found to be in the liquid phase [26]. The periodic image interactions along the confining direction are effectively disabled by using the *slab* command in LAMMPS [27], with a *volfactor* of 3.0. The DFT calculations were done with the SIESTA method [28] using the PBE density functional [29]. We use the TZP basis set for water described in [30]. To assess the accuracy of our simulation setup we determine the polarisability of a water monomer. By applying an external electric field to the monomer and calculating the resulting dipole moment, we obtain a polarisability of 1.6 \AA^3 in Gaussian units, in reasonable agreement with the experimentally reported value of 1.45 \AA^3 [31]. The remaining technical details for both kinds of calculations, classical and DFT, as well as a detailed description of the structural and other properties of the film as obtained in the simulations can be found in Ref. 4.

Figure 2 shows \mathcal{P}_{2D} versus $\mathcal{E}_{\perp}^{\text{ext}}$ for a 2D molecular density of $\sigma = 0.177 \text{ \AA}^{-2}$, for both TIP4P-2005 and DFT calculations. Regarding the orientation of the molecu-

lar dipole moment predicted by the TIP4P/2005 model along the confining direction, two preferential orientations are observed in each water layer (see Supplemental Material). This agrees with the structure reported in previous calculations using first-principles accuracy neural network potentials [9]. The 2D polarisation for the DFT calculations is slightly larger, consistent with the deformation of the electronic cloud. The resulting values of α_{\perp} are shown in Table I, and compared with the results of experiment [1]. For the latter, there is an ambiguity since the actual values of capacitance, \mathcal{P}_{2D} , or α_{\perp} were not reported, but $\epsilon_{\perp} = 2.1$ was given for a range of water film thickness between 8.5 and 15 Å. The α_{\perp} interval appearing in the Table corresponds to that range of film thicknesses. Both theoretical values of α_{\perp} (TIP4P/2005, DFT) fall within the range inferred from experiments ($\alpha_{\perp}^{\text{exp}}$). The inset of Figure 2 also shows the dependence of α_{\perp} on the 2D density of water molecules obtained from the analysis of TIP4P/2005 classical trajectories. These results address the experimental difficulty in ascertaining the experimental pressure conditions [1]. Our results (see Fig. 2) show that α_{\perp} features a very small dependence on the 2D density.

In addition to directly calculable, the proposed 2D polarisability α_{\perp} can be directly obtained from experiment, in particular from capacitance measurements using $l - \alpha_{\perp} = \epsilon_0/C$, where C is the capacitance per unit area, and l is the effective distance between the capacitor plates. This distance is in principle ill-defined at the nanoscale, as the effective width of a plate capacitor depends on the charge distribution around its surface planes[32]. Differential capacitance measurements can be used to avoid the dependence on l , as done in Ref. 1. In particular, by measuring the capacitance with and without dielectric (water), C and C_0 , respectively,

$$\alpha_{\perp} = \Delta l + \epsilon_0(C_0^{-1} - C^{-1}). \quad (2)$$

where Δl is the possible change in inter-plate distance when removing the dielectric (the measured ‘‘sagging’’ [1]). Additionally, such measurements are enough to de-

TABLE I. Two-dimensional normal polarizability of the water film in Å. The experimental value $\alpha_{\perp}^{\text{exp}}$ is obtained from the values of ϵ_{\perp} and w reported in Ref. 1. TIP4P/2005 values ($\alpha_{\perp}^{\text{TIP}}$) were obtained from TIP4P/2005 trajectories under various values of the normal electric field. DFT results correspond to calculations under the same field values on a sample of snapshots of the corresponding TIP4P/2005 classical trajectories ($\alpha_{\perp}^{\text{DFT}}$), or snapshots of classical trajectories for TIP4P/2005 under zero field conditions ($\alpha_{\perp}^{\text{DFT}}$). $(\alpha_{\perp\infty}/\alpha_{\perp})^{\text{exp}}$ corresponds to the ratio of polarisabilities as obtained from $\epsilon = 78$ and $\epsilon_{\infty} = 1.8$ for bulk water.

$\alpha_{\perp}^{\text{exp}}$	$\alpha_{\perp}^{\text{TIP4P}}$	$\alpha_{\perp}^{\text{DFT}}$	$\alpha_{\perp\infty}^{\text{DFT}}$	$(\alpha_{\perp\infty}/\alpha_{\perp})_{\text{film}}^{\text{DFT}}$	$(\alpha_{\perp\infty}/\alpha_{\perp})_{\text{bulk}}^{\text{exp}}$
4.5 – 7.9	5.7	6.1	2.3	0.37	0.45

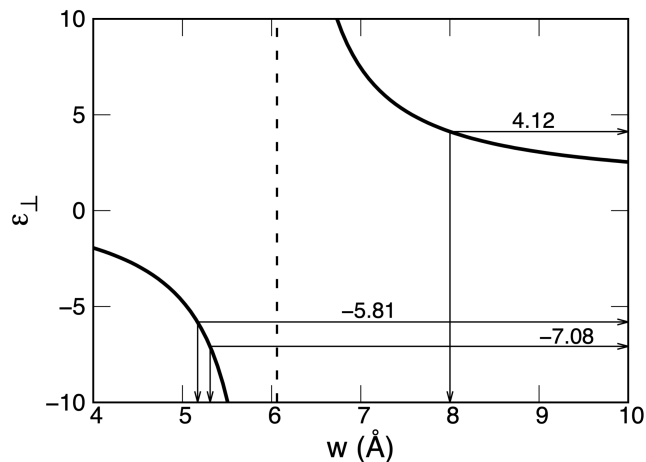


FIG. 3. Dielectric constant across a water thin film as a function of the defined width w of the film for a given value of the 2D polarisability, $\alpha_{\perp} = 6.06$ Å, as obtained with DFT simulations described in the text. Values of ϵ_{\perp} are highlighted for three values of w for the same film: (i) the distance between the origins of the confining potentials $w = 8$ Å, (ii) $w = 5.17$ Å, the accessible perpendicular space as defined by Kumar *et al.* [20], for this bilayer film, and (iii) $w = 5.31$ Å, obtained from normalising the 2D density of the film with the 3D density of bulk water. Negative values for ϵ_{\perp} indicate overscreening, a larger polarisation than what is needed to screen the field completely.

fine an “effective” dielectric constant, $\epsilon_{\perp}^{eff} = \frac{C}{C_0}$, without the need to estimate the effective distance l . ϵ_{\perp}^{eff} represents the overall dielectric behavior of the plate capacitor’s interior, and it is not the dielectric constant of the water film. It can be used to partition the system into layers and evaluate the total capacitance as a model of capacitors in series. But such partitions, particularly the surface ones are still ill-defined and arbitrary.

We illustrate here the extreme sensitivity of ϵ_{\perp} if insisting on defining a water film width w , in spite of the acknowledged arbitrariness of such a choice [9]. The macroscopic formalism is thereby recovered, with α_{\perp} relating to ϵ_{\perp} through [33]

$$\epsilon_{\perp} = \left(1 - \frac{\alpha_{\perp}}{w}\right)^{-1}. \quad (3)$$

ϵ_{\perp} diverges when $w = \alpha_{\perp}$, which nicely points to the physical meaning of the length α_{\perp} : the width of an ideal metal film that would respond with the same polarisability as the one being measured. The divergence is also responsible for the high sensitivity of the value of ϵ_{\perp} to the chosen w . Fig. 3 illustrates that variability for the DFT simulations described above, showing that a given value of α_{\perp} offers dramatically different values of ϵ_{\perp} for different sensible choices of w .

The 2D polarisability α_{\perp} as defined here is an intensive property in the plane (per unit area), but extensive out of plane, and it depends on the amount of substance per

unit area and the 2D density σ . When it is normalized by the experimental density ρ of bulk water at ambient conditions, it gives another effective thickness, $w = \sigma/\rho$, which converges to the film thickness in the macroscopic limit. In our simulations, we obtain $w = 5.31$ Å for the molecular 2D density $\sigma = 0.177$ Å⁻² and $T = 300$ K. We include this thickness in the analysis shown in Fig. 3.

Finally, we address the striking experimental result that the reported dielectric response of the film $\epsilon_{\perp} = 2.1$ is only marginally larger than the electronic dielectric constant of bulk water $\epsilon_{\infty}^b = 1.8$. We calculate the electronic 2D polarizability $\alpha_{\perp\infty}^{DFT}$ of the film by running DFT calculations under different values of $\mathcal{E}_{\perp}^{ext}$ on a sample of snapshots from the zero-field TIP4P/2005 trajectory. The results are shown in Fig. 2 giving the value of $\alpha_{\perp\infty}^{DFT} = 2.3$ Å (Table I), which corresponds to a ratio of $\alpha_{\perp\infty}^{DFT}/\alpha_{\perp}^{DFT}$ of 0.37 for the film. This ratio represents the percentage of electronic to total out of plane polarisability in the film. It can also be estimated for bulk water from experiments as:

$$\left(\alpha_{\infty}^{3D}/\alpha_{\text{bulk}}^{3D}\right)^{\text{exp}} = (1 - \epsilon_{\infty}^{-1})/(1 - \epsilon^{-1}). \quad (4)$$

Using $\epsilon_{\infty}^b = 1.8$ and $\epsilon^b = 78$ the ratio is 0.45, a 40% increase with respect to the thin film. If insisting on keeping the 3D language to discuss the film properties, our result indicates that if $\epsilon_{\perp} = 2.1$ as reported in previous experiments, then $\epsilon_{\perp\infty} = 1.24$ instead of the bulk accepted value 1.8. However, that comparison relies on the experimentally reported value for $\epsilon_{\perp} = 2.1$, which was obtained assuming that the film thickness is well defined. A more appropriate comparison can be established by using the (electronic) molecular polarisability. For the film it is given by normalizing $\alpha_{\perp\infty}^{DFT}$ with the 2D molecular density $\sigma = 0.177$ Å⁻². We obtain a value of 1.01 Å³ in Gaussian units, which is 30% smaller than the experimentally measured molecular polarizability of a water molecule in the gas phase 1.45 Å³ [31] and 37% smaller than the 1.60 Å³ calculated in this work. This reduction is significantly larger than the 4% difference between the molecular polarizability of water in the liquid and gas phases predicted by DFT calculations using the same functional [34] as in this work.

The obtained reduction of the electronic response of the film allows us to conclude that the striking experimental result reported, when properly quantified, is essentially due to the change in the film’s electronic response. We would therefore agree with the comment of Ref. [11] that the reduction in ϵ_{\perp} is not necessarily connected to interfacial water alignment. We show here that the reduction might be connected to changes in electronic polarizability, which have not been considered or addressed in previous works.

That reduction becomes the intriguing result now. The directional dependence of the electronic polarizability

tensor of the water molecule [34] is too small to support the hypothesis of the electronic response reduction being due to prevalent molecular orientations in the film.

The reduction can be related to recent work studying Au-ice nano-capacitors [32, 35] which computed a layer-by-layer α_{\perp} from capacitance measurements using eq.(2). Their results, show that $\alpha_{\perp\infty}$ of the ice layers right at the interface is highly anomalous and anisotropic. While these results are specific for gold capacitors, they indicate that the electronic response of surface layers of water are different from those of the bulk.

Nonetheless, the thickness dependence observed for ϵ_{\perp} remains nicely explained by the capacitors-in-series, dead-layer picture. The point that it is α_{\perp} what is suitable for observation, both experimental and computational, does not invalidate a good phenomenological theory for analysis but care should be exercised when attempting to interpret the experimental behavior in terms of ill-defined experimental observables.

We acknowledge the Basque Government for financial support through grants IT1254-19, IT1584-22 and SGI/IZO-SGIker UPV/EHU for computational resources. Funding from the Spanish MCIN/AEI/10.13039/501100011033 is also acknowledged, through grants PID2019-107338RB-C61 and PID2022-139776NB-C65, as well as a María de Maeztu award to Nanogune, Grant CEX2020-001038-M. MVFS was funded by the U.S. Department of Energy, Office of Science, Basic Energy Sciences, under Award No. DE-SC0019394, as part of the CCS Program. FB thanks the ICL RCS High-Performance Computing facility and the UK Materials and Molecular Modelling Hub, partially funded by the EPSRC (Grant Nos. EP/P020194/1 and EP/T022213/1). We thank Dr. Óscar Pozo for useful discussions.

-
- [1] L. Fumagalli, A. Esfandiari, R. Fabregas, S. Hu, P. Ares, A. Janardanan, Q. Yang, B. Radha, T. Taniguchi, K. Watanabe, *et al.*, *Science* **360**, 1339 (2018).
- [2] N. E. Hill, *Trans. Faraday Soc.* **59**, 344 (1963).
- [3] C. Zhang, F. Gygi, and G. Galli, *J. Phys. Chem. Lett.* **4**, 2477 (2013).
- [4] J. Zubeltzu, F. Corsetti, M. Fernández-Serra, and E. Artacho, *Phys. Rev. E* **93**, 062137 (2016).
- [5] S. De Luca, S. K. Kannam, B. Todd, F. Frascoli, J. S. Hansen, and P. J. Daivis, *Langmuir* **32**, 4765 (2016).
- [6] A. Schlaich, E. W. Knapp, and R. R. Netz, *Phys. Rev. Lett.* **117**, 048001 (2016).
- [7] C. Zhang, *J. Chem. Phys.* **148** (2018), 10.1063/1.5025150.
- [8] G. Monet, F. Bresme, A. Kornyshev, and H. Berthoumieux, *Phys. Rev. Lett.* **126**, 216001 (2021).
- [9] T. Dufils, C. Schran, J. Chen, A. K. Geim, L. Fumagalli, and A. Michaelides, *Chem. Sci.* **15**, 516 (2024).
- [10] F. Deifenbeck and S. Wippermann, *J. Chem. Theo. Comp.* **19**, 1035 (2023).
- [11] J.-F. Olivieri, J. T. Hynes, and D. Laage, *J. Phys. Chem. Lett.* **12**, 4319 (2021).
- [12] M. H. Motevaselian and N. R. Aluru, *ACS Nano* **14**, 12761 (2020).
- [13] V. Ballenegger and J.-P. Hansen, *J. Chem. Phys.* **122**, 114711 (2005).
- [14] D. J. Bonthuis, S. Gekle, and R. R. Netz, *Phys. Rev. Lett.* **107**, 166102 (2011).
- [15] R. Boya, A. Keerthi, and M. S. Parambath, *Physics Today* **77**, 26 (2024), https://pubs.aip.org/physicstoday/article-pdf/77/8/26/20082493/26_1_pt.frik.vxpk.pdf.
- [16] T. Tian, D. Scullion, D. Hughes, L. H. Li, C.-J. Shih, J. Coleman, M. Chhowalla, and E. J. Santos, *Nano Lett.* **20**, 841 (2020).
- [17] L. Colombo, R. Resta, and S. Baroni, *Phys. Rev. B* **44**, 5572 (1991).
- [18] F. Bresme and E. Artacho, *J. Mater. Chem.* **20**, 10351 (2010).
- [19] Both α_{2D} and α_{3D} are rank-two tensors but we are considering one element of the diagonal of the former (α_{\perp}), and the latter is a number times the identity tensor for 3D bulk water.
- [20] P. Kumar, S. V. Buldyrev, F. W. Starr, N. Giovambattista, and H. E. Stanley, *Physical Review E* **72**, 051503 (2005).
- [21] R. Zangi, *Journal of Physics: Condensed Matter* **16**, S5371 (2004).
- [22] C. Calero and G. Franzese, *Journal of Molecular Liquids* **317**, 114027 (2020).
- [23] F. Leoni, C. Calero, and G. Franzese, *ACS Nano* **15**, 19864 (2021).
- [24] S. Han, M. Choi, P. Kumar, and H. E. Stanley, *Nature Physics* **6**, 685 (2010).
- [25] J. L. Abascal and C. Vega, *J. Chem. Phys.* **123** (2005), 10.1063/1.2121687.
- [26] The 2D molecular density range of 0.177 \AA^{-2} - 0.200 \AA^{-2} corresponds to a 3D mass density range of 1.04 g/cm^3 - 1.17 g/cm^3 in Ref.[4].
- [27] A. P. Thompson, H. M. Aktulga, R. Berger, D. S. Bolintineanu, W. M. Brown, P. S. Crozier, P. J. in 't Veld, A. Kohlmeyer, S. G. Moore, T. D. Nguyen, R. Shan, M. J. Stevens, J. Tranchida, C. Trott, and S. J. Plimpton, *Comp. Phys. Comm.* **271**, 108171 (2022).
- [28] J. M. Soler, E. Artacho, J. D. Gale, A. García, J. Junquera, P. Ordejón, and D. Sánchez-Portal, *J. Phys.: Condens. Matter* **14**, 2745 (2002).
- [29] J. P. Perdew, K. Burke, and M. Ernzerhof, *Phys. Rev. Lett.* **77**, 3865 (1996).
- [30] F. Corsetti, M. Fernández-Serra, J. M. Soler, and E. Artacho, *Journal of Physics: Condensed Matter* **25**, 435504 (2013).
- [31] W. M. Haynes, *CRC Handbook of Chemistry and Physics* (CRC press, 2016).
- [32] A. Manino, G. M. Arvelos, K. Kaushik, P. Ordejon, A. R. Rocha, L. S. Pedroza, and M. Fernández-Serra, *In prep* (2024).
- [33] C. Zhang and M. Sprik, *Phys. Rev. B* **93**, 144201 (2016).
- [34] X. Ge and D. Lu, *Phys. Rev. B* **96**, 075114 (2017).
- [35] X. Wen, Q. Ma, A. Mannino, M. Fernandez-Serra, S. Shen, and G. Catalan, *arXiv preprint arXiv:2212.00323* (2023).

Supplemental Material: Redefining the dielectric response of nanoconfined liquids: insights from water

Jon Zubeltzu¹, Fernando Bresme², Matthew Dawber³, María V. Fernández-Serra⁴, and Emilio Artacho^{5,6,7}

¹*Department of Applied Physics, Engineering School of Gipuzkoa, Basque Country University, UPV-EHU, Europa Plaza 1, 20018 San Sebastian, Spain.*

²*Department of Chemistry, Molecular Sciences Research Hub, Imperial College London, London W12 0BZ, United Kingdom and Thomas Young Centre for Theory and Simulation of Materials, Imperial College London, London SW7 2AZ, United Kingdom*

³*Department of Physics and Astronomy, Stony Brook University, New York 11794-3800, USA*

⁴*Department of Physics and Astronomy, Stony Brook University, New York 11794-3800, USA*

⁵*CIC Nanogune BRTA and DIPC, Tolosa Hiribidea 76, 20018 San Sebastian Spain*

⁶*Ikerbasque, Basque Foundation for Science, 48011 Bilbao, Spain*

⁷*Theory of Condensed Matter, Cavendish Laboratory, University of Cambridge, J. J. Thomson Ave, Cambridge CB3 0HE, United Kingdom*

S1: Dipole moment orientation

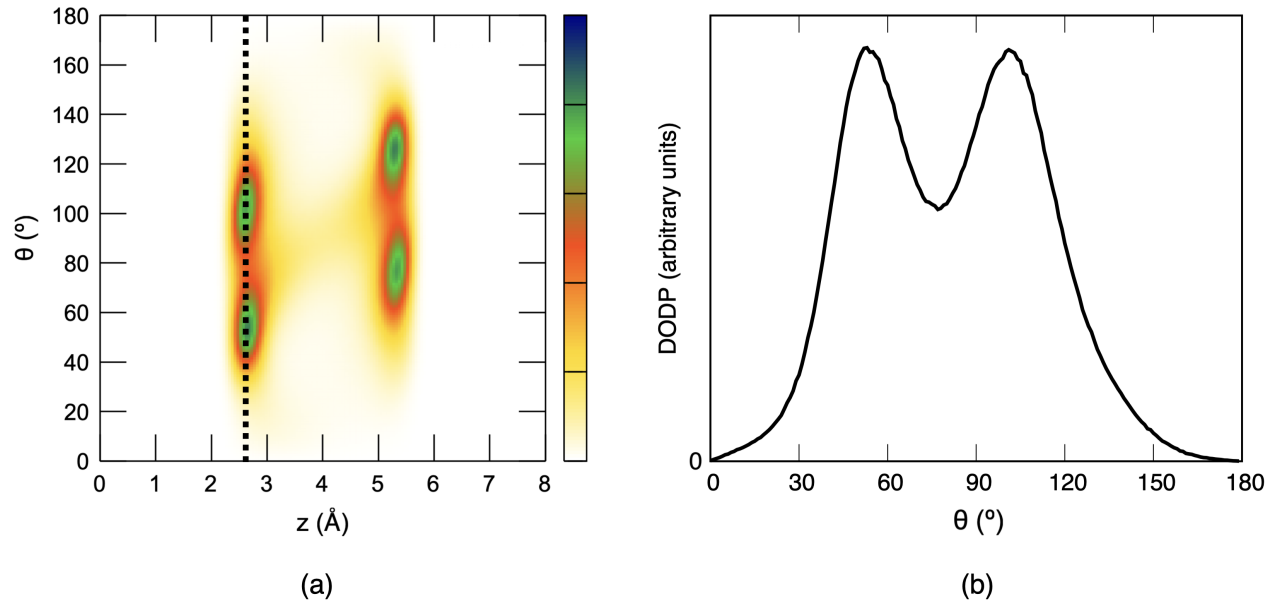


Figure S1: (a) Histogram of dipole moment orientations of water molecules along the confining direction for the TIP4P/2005 model. (b) Dipole orientation distribution profile of water molecules at $z = 2.6$ Å (indicated by the dashed vertical line in (a)).

Figure S1(a) presents the histogram of dipole moment orientations of water molecules relative to the positive direction of the z -axis (the confining direction) for the TIP4P/2005 model in the absence of an external electric field. Figure S1(b) displays the dipole orientation distribution profile (DODP) for the same water molecules at $z = 2.6$ Å, corresponding to the dashed vertical line in Figure S1(a).